Content Delivery Analysis in Cellular Networks With Aerial Caching and mmWAVE Backhaul

Wei Wang, *Member, IEEE*, Nan Cheng, *Member, IEEE*, Yiliang Liu, *Member, IEEE*, Haibo Zhou, *Senior Member, IEEE*, Xiaodong Lin, *Fellow, IEEE*, and Xuemin Shen, *Fellow, IEEE*

***Abstract*—In this paper, we investigate the successful content delivery (SCD) performance in the unmanned aerial vehicle (UAV) integrated terrestrial cellular networks, where the caching-enabled UAVs are dispatched to offload the burst traffic from the cellular networks. Specifically, the UAV and terrestrial cellular network share the same spectrum resources for user downlink communications and each UAV uses millimeter wave (mmWave) communications for self-backhaul. We derive a closed-form expression of the achievable rate of the mmWave wireless backhaul link and then analyze the minimum cache hit probability to achieve a certain backhaul rate requirement. By approximating the general probabilistic line-of-sight (LoS) propagation model as a LoS ball model, we analyze the conditional SCD probabilities by leveraging stochastic geometry tools. Simulation results demonstrate that the UAV integrated cellular network can not only provide more access opportunities but also achieve higher SCD performance than the conventional terrestrial network for ground users. Moreover, there exists an optimal UAV density and height to maximize the SCD performance. Our results provide useful guidelines for the design and deployment of future UAV-assisted networks.**

***Index Terms*—Unmanned aerial vehicle (UAV) communications, caching, mmWave backhaul, stochastic geometry.**

I. Introduction

DUE to the high mobility and flexible deployment capability, unmanned aerial vehicles (UAVs) have plenty of potential applications for various industrial and emergency services [1]. By mounting communication devices on the UAV, communication services can be achieved in a more economical and flexible manner in some special scenarios with temporal burst traffic demands, such as sport events, assembly, etc. [2]–[5], or communications rehabilitation in disaster areas [6]. To support the UAV-assisted communications, a high throughput wireless backhaul link must be built through which UAV can access the core network, which is very challenging due to the long range propagation loss and scarce spectrum resources. Fortunately, millimeter wave (mmWave) technologies shaped in the fifth-generation (5 G) communications greatly expand radio resources, and the line-of-sight (LoS) propagation between UAV and the terrestrial base stations (TBSs) makes mmWave communications particularly suitable for UAV-TBS backhaul [7]–[9]. With antenna arrays at TBSs, high antenna gain beams can be created to compensate the severe propagation loss. Therefore, mmWave communications provide a rich of opportunities for UAV-assisted communications. Moreover, by caching the most popular contents at each UAV according to the users' interests, the caching-enabled UAVs can facilitate traffic offloading and content delivery in congestion areas[1] without frequent backhaul requests, which significantly reduces the backhaul load and promotes the UAV-assisted communications in practical scenarios [10].

In this paper, we investigate the UAV-assisted content delivery by considering the effect of both the mmWave backhaul and edge caching. We analyze the successful content delivery (SCD) performance defined as the successful probability of delivering a certain amount of data within a given time period, and evaluate the impact of key parameters, such as the altitude and density of UAV and the cache size, on the SCD performance. Particularly, we aim to explore the following two problems:

- How much performance gain can be achieved by integrating UAVs into cellular networks in terms of SCD?
- How will the mmWave backhaul and finite cache affect the SCD performance?

A. Prior Work and Motivation

The coverage and rate performance of UAV-assisted communications have been investigated in existing works in [2], [7],

Manuscript received January 29, 2021; accepted April 19, 2021. Date of publication April 22, 2021; date of current version June 9, 2021. This work was supported in part by the National Natural Science Foundation of China under Grant 62001220, in part by the Natural Science Foundation of Jiangsu Province under Grant BK20200440, in part by the Fundamental Research Funds for the Central Universities under Grants 1004-YAH20016 and NT2020009, and in part by the Natural Sciences and Engineering Research Council (NSERC) of Canada. The review of this article was coordinated by Dr. Xiaodai Dong. *(Corresponding authors: Wei Wang; Yiliang Liu.)*

Wei Wang was with the Department of Electrical and Computer Engineering, University of Waterloo, Canada . He is now with the College of Electronic and Information Engineering, Nanjing University of Aeronautics and Astronautics, Nanjing 211106, China (e-mail: wei_wang@nuaa.edu.cn).

Nan Cheng is with the School of Telecommunications Engineering, Xidian University, Xian 710071, China, and also with the State Key Lab of ISN, Xidian University, Xian 710071, China (e-mail: dr.nan.cheng@ieee.org).

Yiliang Liu is with the School of Cyber Science and Engineering, Xi'an Jiaotong University, Xi'an 710049, China (e-mail: alanliuyiliang@gmail.com).

Haibo Zhou is with the School of Electronic Science and Engineering, Nanjing University, Jiangsu 210023, China (e-mail: haibozhou@nju.edu.cn).

Xiaodong Lin is with the School of Computer Science, University of Guelph, Guelph, ON N1G 2W1, Canada (e-mail: xlin08@uoguelph.ca).

Xuemin Shen is with the Department of Electrical and Computer Engineering, University of Waterloo, Waterloo, ON N2L3G1, Canada (e-mail: sshen@uwaterloo.ca).

Digital Object Identifier 10.1109/TVT.2021.3074991

[1]The service demand of the cellular network may suffer an abrupt increase due to the temporal events, and UAVs can be sent to such areas to offload the traffic from the cellular network.

[11]–[18]. In [2], the authors analyzed the coverage performance in the aerial underlay terrestrial cellular system, where the UAV is employed to provide coverage for temporary events. Based on the probabilistic LoS channel model, the coverage and rate performance of UAV-based communications with underlaid device-to-device (D2D) users was analyzed in [13]. It is shown that the optimal altitude of UAV decreases with the density of D2D users. The coverage performance in UAV-assisted networks was also derived in [15] using a general probabilistic LoS and non-line-of-sight (NLoS) propagation channel model. The coverage performance of energy harvesting-powered caching UAVs assisted terrestrial cellular networks was analyzed by deriving the successful transmission probabilities in [16], and the optimal average altitude was analyzed to maximize the coverage performance. The impact of the height and density of UAV on the spatial throughput of a downlink UAV integrated terrestrial cellular network was also analyzed in [17], which shows that there exists a critical UAV density to maximize the spatial throughput.

To support the UAV-assisted communications, a dedicated wireless backhaul link must be built in a reliable and efficient manner to connect the UAVs into the core network. The feasibility of using long-term evolution (LTE) networks for UAV backhaul was discussed in [19], and the impact of UAV altitude on the backhaul throughput was also evaluated. Since the BS antennas are down tilted to support ground users in cellular networks, UAV can only be served through the side lode, causing high antenna gain loss. In addition, the UAV may receive more interference from nearby BSs due to the LoS propagation environment, resulting in severe capacity degradation. To improve the throughput of backhaul links, mmWave communications [20] has been used for UAV backhaul by exploiting the vast available spectrum. While the A2G LoS channel property promotes the application of mmWave technology for the UAV-BS backhaul, the interference between the backhaul and access links can be avoided as well. Moreover, by adopting mmWave antenna arrays at TBS, 3D beams can be created up towards the UAV, which significantly improves the UAV-BS antenna gain. A prototype and field test of UAV mmWave communications have been demonstrated in a more recent result [21].

Considering the hardware cost and complexity in mmWave communications, the number of simultaneously served backhaul requests is usually limited due to the limited radio-frequency (RF) chain. To mitigate the backhaul load, edge caching has been proposed for small-cell networks in the latest third Generation Partnership Project (3GPP) standards [22]. When the requested content from users is stored at the local cache, it can be directly transmitted to such users without fetching from the core network through the backhaul. In this way, both the backhaul load and delay can be significantly reduced [23]–[25]. Thus, edge caching has been regarded as a promising solution to mitigate the backhaul requirement in the UAV-assisted communications [16].

The limited caching and mmWave backhaul unavoidably incur extra transmission delay, which has not been characterized in previous coverage performance evaluations in [2], [15], [17]. To capture the effect of transmission delay in the UAV integrated cellular network, we evaluate the SCD performance considering the unique A2G channel model and the interference between the aerial links (UAV to ground users (UEs)) and terrestrial links (TBS to UEs). Nevertheless, it is a challenging task to derive the SCD probability expression. Moreover, the impact of mmWave backhaul and limited caching on the SCD performance remains unclear, which motivates this work.

B. Contributions and Organization

In this paper, we consider a general framework of a caching-enabled UAV integrated cellualar network with mmWave backhaul, where the positions of the terrestrial BSs and UAVs are modeled as independent Homogeneous Poisson Point Process (HPPP) and Poisson Hardcore Process, respectively. In particular, the aerial and terrestrial downlink communication links share the same spectrum resources and the UAVs connect to the TBS with mmWave backhaul. The contributions of this paper are summarized as follows.

- We derive a closed-form expression of the average achievable rate of the mmWave backhaul under both general case and noise-limited case, and derive the minimum backhaul delivery time that determines the conditional SCD probability under cache miss case. In addition, the minimum cache hit probability for a given backhaul rate requirement is also analyzed.
- We derive closed-form expressions of the approximated conditional SCD probabilities, by approximating the probabilistic LoS propagation A2G channel model as the LoS ball model. The impact of the height and density of the UAV on the conditional SCD probability is also analyzed.
- We evaluate the impact of different parameters on the SCD performance. It shows that there exists an optimal height and density of UAV that maximizes the SCD probability. For a small value of UAV density, the SCD performance of the caching-enabled UAV integrated network is comparable with that of the infinite backhaul case.

The remainder of this paper is organized as follows. We describe the system model in Section II. The average achievable rate of the mmWave wireless backhaul is analyzed in Sections III, followed by the conditional SCD probabilities under TBS or UAV association in Sections IV. We present the simulation results in Section V and conclude this paper in Section VI.

Notation: Bold symbols in capital and lower-case letter denote matrices and vectors, respectively. $[\cdot]^T$, $[\cdot]^\dagger$, and $[\cdot]^H$ denote the transpose, conjugate, and conjugate transpose operations, respectively. $|\cdot|$, $\|\cdot\|$, and $\mathbb{P}(\cdot)$ represent absolute value, Euclidean norm, and probability, respectively. $\mathcal{CN}(\mu, \sigma^2)$ denotes complex Gaussian distribution with mean μ and variance σ^2. $\|\cdot\|_1$ is the l_1 induced matrix norm, i.e., $\|\mathbf{A}\|_1 = \max_{1\le j\le n} \sum_{i=1}^{m} |a_{ij}|$. Specifically, $\varphi_0(\alpha, x) = {}_2F_1(\alpha, \alpha+\delta; \alpha+1+\delta; -x^{-1})$, $\varphi_i(\alpha, x) = {}_2F_1(\alpha+i, i-\delta; i-\delta+1; -x)$ are used in this paper, with ${}_2F_1(\cdot)$ being the Gauss hypergeometric function, $\delta_s = 2/\alpha_s$, $s \in \{B, L, N, m\}$, and $V_n \triangleq \Gamma(n+\delta)\Gamma(1-\delta)/\Gamma(n)$ with $\Gamma(\cdot)$ being the gamma function.

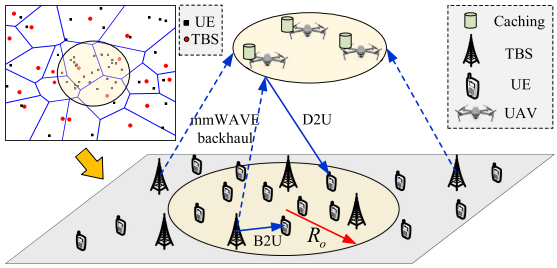

Fig. 1. The caching enabled UAV integrated terrestrial networks with mmWave backhaul.

II. System Model

We consider UAV-assisted downlink communications, where the terrestrial network encounters an abrupt increase of cellular service demands that appear in a specific region due to temporary events, such as traffic jamms or emergency conditions. As shown in Fig. 1, the congestion area is denoted by the heavy-shaded circular area with radius R_o. The caching-enabled UAVs are dispatched to such area[2] to provide enhanced network service performance for UEs within this area. For system level performance evaluation, as assumed in the literature, we assume that the positions of the TBSs is distributed according to a HPPP Φ_B with intensity λ_B, and the positions of UAVs are modeled as a Matérn Hardcore Process Φ_D with intensity λ_D since UAVs are prohibited to be closer than a fixed safe distance R_{safe} for flight safety. Each user can connect either to the TBS or the UAV opportunistically with the nearest association rule. Particularly, the UAV and TBS share the same spectrum band operating at sub-6 GHz band for UE downlink content delivery,[3] and each TBS is equipped with N antennas and each UAV is equipped with a single antenna due to its size limitation. For the UAVs, we consider that each UAV connects to the nearest TBS for wireless backhaul through mmWave communications. Moreover, to alleviate the backhaul requirement of UAVs, each UAV has a finite cache that can store popular contents. When the requested contents from UE is stored at the UAV's cache, it can directly transmit to the UE, otherwise such content will be delivered from the TBS through the mmWave communications. Note that, to facilitatethe analysis, we assume that all the UAVs are flying at the same altitude H_D, and all the TBSs have the same height H_B.

A. Channel Model

In the UAV integrated terrestrial cellular network, two types of communication links are considered, i.e., the terrestrial link and aerial link.

1) TBS-to-UE Channel Model: We assume that all terrestrial links undergo independent and identically distributed (i.i.d.) Rayleigh fading together with a large-scale path loss with a path loss exponent $\alpha_B > 2$. The channel from the ith TBS to the kth user in the jth cell is expressed as $\mathbf{h}_{ijk} = \sqrt{L(|X_{ijk}|)}\mathbf{u}_{ijk}$, where $L(|X_{ijk}|)$ and $\mathbf{u}_{ijk} \in \mathbb{C}^{1\times N}$ denote the corresponding path loss and small-scale Rayleigh fading with $\mathbf{u}_{ijk} \sim \mathcal{CN}(\mathbf{0}, \mathbf{I})$. Note that $L(|X_{ijk}|) = c_B|X_{ijk}|^{-\alpha_B}$, where c_B is a constant path loss, with $|X_{ijk}|$ being the corresponding distance.

2) Drone-to-UE Channel Model: For the Drone-to-UE aerial channel, both the LoS and NLoS links are considered and the Signomial model is usually adopted to characterize the propagation condition [16]. The LoS probability is given by [7]

$$\mathbb{P}_{L,a}(r) = \frac{1}{1 + C_a \exp(-B_a(\theta_a - C_a))}, \tag{1}$$

where B_a and C_a are constant values depending on the environment, θ_a is the elevation angle with $\theta_a = \arcsin(\frac{H_D}{|Y_{ljk}|})$, and $|Y_{ljk}|$ is the distance from the lth UAV to the kth user in the jth cell. Due to the lower probability of multipath fading in aerial channel, the small scale fading is ignored as has been assumed in [13], [14]. Then, the Drone-to-UE channel from the lth UAV to the kth user in the jth cell is given by

$$L_a(|Y_{ljk}|) = \begin{cases} c_L\,|Y_{ljk}|^{-\alpha_L}, & \text{for LoS link,} \\ c_N\,|Y_{ljk}|^{-\alpha_N}, & \text{otherwise,} \end{cases} \tag{2}$$

where c_L, α_L, c_N, and α_N are the path loss at a reference distance and the path loss exponent for the LoS link and NLoS link, respectively.

3) TBS-to-Drone Mmwave Backhaul Channel Model: For the mmWave backhaul link, a similar blockage channel model is adopted with the LoS link probability given by

$$\mathbb{P}_{L,b}(|Z_{jl}|) = \frac{1}{1 + C_b \exp(-B_b(\theta_b - C_b))}, \tag{3}$$

where B_b, C_b, and θ_b are defined similarly with that in (1), $\theta_b = \arcsin(\frac{H_D}{|Z_{jl}|})$ with $|Z_{jl}|$ being the distance between the lth UAV and the jth TBS. Since the UAV is hovering at a relatively high altitude and the TBS to UAV link will be in LoS with high probability due to the less scatering, meanwhile the effect of LoS link is dominant over NLoS link as indicated in [26], only the LoS path is considered in this case. Then, the path loss between the jth TBS and the lth UAV is given by

$$L_b(|Z_{jl}|) = c_M\,|Z_{jl}|^{-\alpha_M}, \tag{4}$$

where c_M and α_M are the path loss at a reference distance and the path loss exponent, respectively. Note that the small-scale fading is ignored in this case, as it has been proven that the small-scale fading will induce minor impact in mmWave cellular systems [27], [28].

To support reliable and high data rate backhaul, both the TBS and UAV are equipped with antenna array and form directional beams. Specifically, similar to the assumptions in [29], we assume that each UAV has a directional antenna, which has horizontal and vertical beamwidth θ_D and rectangular radiation pattern, with main lobe antenna gain G_D and side lobe gain g_D. Then the beam of each UAV will illuminate an ring sector area with arc angle θ_D in the ground, only within which the UAV can be served or interfered.

[2]The GPS location information of the burst traffic areas can be collected and sent to the assigned UAVs in advance.

[3]This assumption allows users to access the TBS or UAV without any modification of their devices. In addition, the quality of service for the UAV to user link can be guaranteed with the shared licensed spectrum.

For the mmWave antenna at the TBS, similar to [29], we assume that each TBS uses uniform planar square array (UPA) forming a directional beam with beamwidth θ_B in both azimuth and elevation, and gain of G_B inside the main lobe and g_B otherwise. For the intended communication link, we assume that the angle-of-arrival can be obtained accurately, and thus the intended UAV receiver can steer the antenna to maximize the antenna gain. Hence, the antenna gain for the intended link is always $G_B G_D$, but that of the interfering link varies independently and randomly. With the antenna pattern above, the antenna gain of an interfering links for the mmWave backhaul communication is given by

$$G_I = \begin{cases} G_B G_D, & \text{with Prob. } p_{I_1} = B_m D_m, \\ G_B g_D, & \text{with Prob. } p_{I_2} = B_m(1-D_m), \\ g_B G_D, & \text{with Prob. } p_{I_3} = (1-B_m)D_m, \\ g_B g_D, & \text{with Prob. } p_{I_4} = (1-B_m)(1-D_m), \end{cases} \tag{5}$$

where $B_m = \frac{\theta_B}{2\pi}\frac{\theta_B}{\pi} = \frac{\theta_B^2}{2\pi^2}$, $D_m = \frac{\theta_D}{2\pi}\frac{\theta_D}{\pi} = \frac{\theta_D^2}{2\pi^2}$.

B. Content Placement

The content is cached based on the popularity. We assume that the total content is equally divided into T files, denoted as $\mathcal{F} := \{f_1, \ldots, f_i, \ldots, f_T\}$, where f_i is the ith most popular content. The request probability of the ith most popular content is modelled by the well-known Zipf distribution, given by

$$p_i = \frac{i^{-\kappa}}{\sum_{l=1}^{T} l^{-\kappa}}, \tag{6}$$

where κ is the Zipf exponent standing for the popularity skewness. We adopt the most popular contents (MPC) caching strategy, and then the cache hit probability that UE's requested content is stored at the UAV is denoted as $q_{\text{hit}} = \sum_{i=1}^{L} p_i$ [25], where $L \leq T$ is the cache size. Then, the set of UAVs can be divided into two independent processes based on the thinning theroem, i.e., the UAVs without backhaul links Φ_D^a with intensity $\lambda_D q_{\text{hit}}$ and the UAVs with backhaul links Φ_D^b with intensity $\lambda_D(1-q_{\text{hit}})$.

C. Data Transmission Model

We assume that the TBSs and UAVs share the whole spectrum for user downlink communications with a total bandwidth of W, and the bandwidth of the mmWave backhaul link is W_M. With multiple antennas at the TBSs, each TBS can serve K UEs simultaneously using space-division multiplex access (SDMA) techniques. To mitigate the intra-cell interference, each TBS adopts zero-forcing beamforming (ZFBF) scheme with beamforming vector given by

$$\mathbf{W}_i = \mathbf{H}_i^H (\mathbf{H}_i \mathbf{H}_i^H)^{-1}, \tag{7}$$

where $\mathbf{H}_i = [\mathbf{h}_{ii0}^H, \ldots, \mathbf{h}_{ii(K-1)}^H]^H$. Note that the kth column of $\mathbf{W}_i$ corresponds to the beamforming vector of the ith TBS to the kth user. For the single antenna UAVs, we consider each UAV can serve K_d users through time-division multiplex access (TDMA). Due to the caching capability, only those UAVs with uncached contents request will use the mmWave backhaul link, and thus those TBSs without any backhaul requests will keep inactive. The probability that a TBS being active for backhaul transmission is denoted by p_a, which can be given by (8) under the nearest BS association scheme [30], [31].

$$p_a = 1 - \left(1 + \frac{\lambda_D(1-q_{\text{hit}})}{3.5\lambda_B}\right)^{-3.5}. \tag{8}$$

Denote the number of UAVs that request backhaul transmission from the jth TBS as N_j, and the TBS will serve the N_j requests through frequency-division multiplex access (FDMA). Then, the achievable rate of the typical mmWave link is given by

$$R_b = \frac{W_M}{N_o} \log_2(1 + \text{SINR}_b), \tag{9}$$

where

$$\text{SINR}_b = \frac{P_m G_S L_b(|Z_{00}|)}{\sum_{j \in \Phi_B^a \setminus \{0\}} P_m G_j L_b(|Z_{j0}|) + \sigma_m^2}, \tag{10}$$

where N_o is the backhaul load of the typical TBS, Φ_B^a denotes the set of active TBSs with backhaul requests, and σ_m^2 is the noise power of the mmWave receiver.

D. Performance Metrics

To characterize the effect of wireless backhaul on the coverage performance, the SCD probability is adopted as the performance metric in this work, which characterizes the probability of successfully delivering Q bits within a time period τ, i.e., $\mathcal{P}_{SCD} = \mathbb{P}(R \geq \frac{Q}{\tau})$. Based on different user association cases, the SCD probability can be expressed as

$$\mathcal{P}_{SCD} = \mathcal{A}_B \mathcal{P}_{SCD}^B + \mathcal{A}_D \mathcal{P}_{SCD}^D, \tag{11}$$

where $\mathcal{A}_B$ and $\mathcal{A}_D$ are the association probabilities to the terrestrial BS and UAV, respectively, with $\mathcal{P}_{SCD}^B$ and $\mathcal{P}_{SCD}^D$ being the corresponding conditional SCD probability. Note that $\mathcal{P}_{SCD}^D = q_{\text{hit}} \mathcal{P}_{SCD}^{D,\text{hit}} + (1-q_{\text{hit}}) \mathcal{P}_{SCD}^{D,\text{miss}}$, where $\mathcal{P}_{SCD}^{D,\text{hit}}$ and $\mathcal{P}_{SCD}^{D,\text{miss}}$ denote the conditional SCD probability under cache hit and cache miss cases, respectively, when the UE is associated with UAVs.

III. Average Rate of the Mmwave Backhaul

We first evaluate the achievable backhaul rate in this section. Consider a typical UAV that requires mmWave backhaul, the probability density function (PDF) of the nearest distance of a typical backhaul link r_v is given by

$$f_{r_v}(r) = 2\pi\lambda_B r e^{-\pi\lambda_B(r^2 - H_\Delta^2)}, r > H_\Delta, \tag{12}$$

where $H_\Delta = H_D - H_B$. Then, based on the lemma in [32], [33], we can derive the average backhaul rate, which is given as follows.

Theorem 1: The average rate of the typical mmWave backhaul is given by

$$\bar{R}_b = \frac{W_M}{\ln 2\, N_o} \int_0^\infty \int_{H_\Delta}^\infty \frac{1 - e^{-\frac{z P_m G_S c_M}{r^\alpha M}}}{z e^{z\sigma_m^2}} e^{\frac{\pi\lambda_B p_a \Theta r^2}{2}} f_{r_v}(r) dr dz, \tag{13}$$

where Θ is given by the following two cases:

when $\alpha_M > 2$, we have

$$\Theta = {}_2F_1\left(-\delta_m, N_v; 1-\delta_m; -\frac{zP_m\bar{G}_I c_M}{N_v r^{\alpha_M}}\right) - 1, \quad (14)$$

when $\alpha_M = 2$, we have

$$\Theta = \frac{\left(\frac{N_v r^2}{zP_m\bar{G}_I c_M}\right)^{N_v} {}_2F_1\left(N_v, N_v+1; N_v+2, -\frac{N_v r^2}{zP_m\bar{G}_I c_M}\right)}{N_v+1} - 1. \quad (15)$$

In addition, N_v is a constant used for approximation and $\bar{G}_I$ is the average value of G_I, which can be calculated by (5).

Proof: See Appendix A. ■

For mmWave communications, it has been shown through various simulations and measurements that mmWave networks tends to be noise-limited, which is different with conventional cellular networks, see [28], [34] and references therein. Then, for the noise limited case, we have the following corollary.

Corollary 1: The average rate of the typical mmWave backhaul under the noise limited case is given by

$$\bar{R}_b = \frac{W_M}{\ln 2\, N_o}\int_0^\infty \int_{H_\Delta}^\infty \frac{1-e^{-zP_m G_S c_M}}{z e^{z\sigma_m^2 r^{\alpha_M}}} f_{r_v}(r) dr dz. \quad (16)$$

Specifically, when $\alpha_M = 2$, we can derive a closed-form upper bound given by

$$\bar{R}_b \le \frac{W_M}{\ln 2\, N_o}\frac{\pi\lambda_B P_m G_S c_M}{\sigma_m^2}\left(-\mathrm{Ei}(-\pi\lambda_B H_\Delta^2)\right) \triangleq \bar{R}_b^U, \quad (17)$$

where $\mathrm{Ei}(x) = \int_{-\infty}^x \frac{e^t}{t}dt$, $x<0$, is the exponential integration defined in [35].

Proof: Following the proof in Appendix A, the average mmWave backhaul rate under noise limited case can be derived. When $\alpha_M = 2$, (16) can be further simplified as

$$\begin{aligned}\bar{R}_b &= \frac{W_M}{\ln 2\, N_o}\int_0^\infty \frac{1-e^{-zP_m G_S c_M}}{z e^{z\sigma_m^2 H_\Delta^2}}\frac{\pi\lambda_B}{\pi\lambda_B + z\sigma_m^2} dz \\ &\overset{(a)}{\le} \frac{W_M}{\ln 2\, N_o}\int_0^\infty \frac{\pi\lambda_B P_m G_S c_M}{\pi\lambda_B + z\sigma_m^2} e^{-z\sigma_m^2 H_\Delta^2} dz,\end{aligned} \quad (18)$$

where step (a) follows from that $f(x) = \frac{1-e^{-ax}}{x}$ is a monotonically decreasing function for any positive value of a, and $\lim_{x\to 0} e^{-x} = 1-x$. ■

We can observe from (16) that, for the noise limited case, the average rate is a decreasing function of the path loss exponent of the mmWave link. Thus, the transmission rate of the mmWave backhaul is upper bounded by (17), and the minimum time required for delivering Q bits from the serving TBS to the typical UAV can be derived

$$T_b \ge \frac{\ln 2\, N_o Q\sigma_m^2}{\pi\lambda_B P_m G_S c_M W_M\left(-\mathrm{Ei}(-\pi\lambda_B H_\Delta^2)\right)}. \quad (19)$$

We can see from (19) that the delivering time can be reduced by decreasing the altitude of the UAV. Moreover, from (17), we can observe that for fixed density of TBS, to guarantee the minimum backhaul rate, $R_{b,\min}$, the number of UAVs being simultaneously served by a TBS for wireless backhaul should not exceed a maximum number, which further incurs the minimum requirement for the cache as follows.

Corollary 2: To meet a given minimum backhaul rate requirement, the cache hit probability should satisfy

$$q_{\text{hit}} \ge 1 - \frac{\pi\lambda_B^2 W_M P_m G_S c_M}{\ln 2\lambda_D \sigma_m^2 R_{b,\min}}\left(-\mathrm{Ei}(-\pi\lambda_B H_\Delta^2)\right). \quad (20)$$

Proof: Based on (17), we can obtain the maximum mmWave backhaul load for a TBS, since the mean load of mmWave backhaul is given by $(1-q_{\text{hit}})\lambda_D/\lambda_B$, we can obtain (20). ■

IV. Successful Content Delivery Probability Analysis

In the following, we will analyze the conditional SCD performance of a typical user located at the origin of the coordinate system, which presents the general results for other users according to Slivnyak's theorem [36]. Each user is associated to the nearest TBS.

For ease of expression, let r_b and r_d denote the nearest distance between the typical user to the serving TBS and UAV, respecrively, i.e., $r_b = |X_{000}|$ and $r_d = |Y_{000}|$. By using the void probability of PPP, the cumulative distribution function (CDF) of R_s can be given by

$$F_{r_s}(r) = 1 - \exp(-\pi\lambda_s(r^2 - H_s^2)), r > H_s, s \in \{b, d\}. \quad (21)$$

Then the association probability can be derived as follows.

Lemma 1: The probability that a typical user is associated with the TBS is given by

$$\mathcal{A}_B = 1 - \frac{\lambda_D}{\lambda_B+\lambda_D} e^{-\pi\lambda_B(H_D^2 - H_B^2)}, \quad (22)$$

and the probability that a typical user is associated with the UAV is $\mathcal{A}_D = 1 - \mathcal{A}_B$.

Proof: Under the nearest BS association rule, we have

$$\begin{aligned}\mathcal{A}_B &= \mathbb{P}(r_b < r_d) \\ &= \int_{H_D}^\infty \left(1 - e^{-\pi\lambda_B(r^2 - H_B^2)}\right) f_{r_d}(r) dr \\ &= 1 - \int_{H_D^2}^\infty \pi\lambda_D e^{-\pi\lambda_D(r-H_D^2)} e^{-\pi\lambda_B(r-H_B^2)} dr.\end{aligned} \quad (23)$$

Then (22) can be obtained. ■

Then, the conditional distribution of the nearest serving distance can be derived as follows.

Lemma 2: The CDF of the nearest distance between the typical user and TBS, under the condition that the typical user is associated to TBS, is given by

$$F_{r_b|B}(r) = \begin{cases} \frac{1}{\mathcal{A}_B}\left(1 - e^{-\pi\lambda_B(r^2 - H_B^2)}\right), H_B \le r \le H_D, \\ \vartheta_0 + \vartheta_1\left(e^{-\pi\lambda_0 H_D^2} - e^{-\pi\lambda_0 r^2}\right), r > H_D, \end{cases} \quad (24)$$

where $\vartheta_0 = \frac{1-e^{-\pi\lambda_B(H_D^2 - H_B^2)}}{\mathcal{A}_B}$, $\vartheta_1 = \frac{\lambda_B e^{\pi(\lambda_B H_B^2 + \lambda_D H_D^2)}}{\mathcal{A}_B\lambda_0}$, $\lambda_0 = \lambda_B + \lambda_D$. Moreover, the CDF of the nearest distance from the typical user to the UAV conditioning that the typical user is

associated with UAV is given by

$$F_{r_d|D}(r) = \tilde{\vartheta}_1 \left(e^{-\pi\lambda_0 H_D^2} - e^{-\pi\lambda_0 r^2} \right), r \geq H_D, \tag{25}$$

with $\tilde{\vartheta}_1 = \frac{\lambda_D}{\mathcal{A}_D \lambda_0} e^{\pi(\lambda_B H_B^2 + \lambda_D H_D^2)}$.

Proof: See Appendix B. ■

A. UE Associated With the TBS

When the typical user is connected to TBS, the received signal-to-interference-plus-noise ratio (SINR) at the typical user is given by

$$\gamma_{B,0} = \frac{\frac{P_B}{K} |\mathbf{h}_{000}\mathbf{w}_{00}|^2 L(r_b)}{I_B + I_D + \sigma^2}, \tag{26}$$

where $\mathbf{w}_{00}$ is the beamforming vector of the tagged TBS for the typical user, σ^2 is the received noise power, and the interference term is given by

$$I_B = \sum_{i \in \Phi_B \setminus \{0\}} \sum_{k=0}^{K-1} \frac{P_B}{K} |\mathbf{h}_{i00}\mathbf{w}_{ik}|^2 L(|X_{i00}|), \tag{27}$$

and

$$I_D = \sum_{i \in \Phi_D} P_D L_a(|Y_{i00}|). \tag{28}$$

Denote $I = I_B + I_D$, Then, the conditional SCD can be calculated by

$$\begin{aligned} \mathcal{P}_{SCD}^B &= \mathbb{P}(R \geq \frac{Q}{\tau}) \\ &= \mathbb{P}(\gamma_{B,0} \geq \bar{\gamma}) \\ &\overset{(b)}{\approx} \mathbb{P}\left(|\mathbf{h}_{000}\mathbf{w}_{00}|^2 \geq sI \right) \\ &\overset{(c)}{=} \sum_{m=0}^{M-1} \mathbb{E}_{r_b} \mathbb{E}_I \left[\frac{s^m I^m}{m!} e^{-sI} \right], \end{aligned} \tag{29}$$

where $\bar{\gamma} = 2^{Q/\tau} - 1$, $s = \frac{\bar{\gamma} K}{P_B c_B} r_b^{\alpha_B}$. In step (b), the noise effect is ignored as compared with the interference, (c) holds due to the fact that $|\mathbf{h}_{000}\mathbf{w}_{00}|^2 \sim \text{Gamma}(M, 1)$. Due to the high order term in (29) and the probabilistic propagation model in (1), it is cumbersome to derive the closed-form expression of the Laplace transform of the interference. To facilitate the analysis, we adopt the LoS ball model with radius $R_{\mathcal{B}}$, where the LoS probability of a certain link is one when the distance is less than $R_{\mathcal{B}}$, and zero otherwise [37]. From (1), we can find that the radius is dependent on the height of the UAV, but the exact value of $R_{\mathcal{B}}$ can only be obtained through one-dimensional searching at the moment.[4] As shown in Fig. 2, we evaluate the average received aggregate interference power using the probability model in (1) and the LoS ball model, where the radius is obtained through numerical searching under the given system settings in Section V. We can observe that the average received aggregate interference power with the two models match well, which validates the accuracy

[4]Note that $R_{\mathcal{B}}$ is usually much smaller than the size of the burst traffic area R_o, thus the upper bound of the LoS link is denoted as $R_{\mathcal{B}}$ in the subsequent analysis.

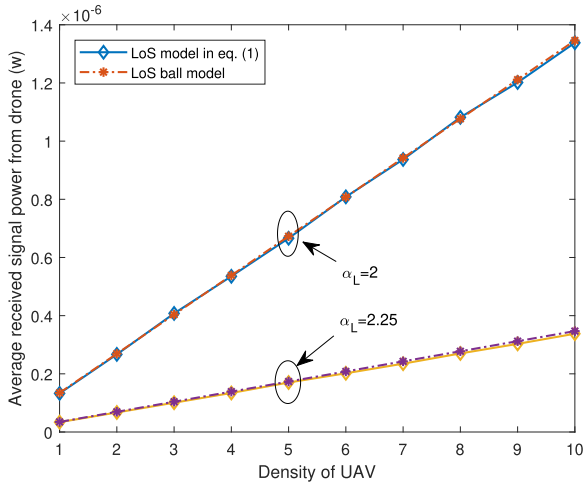

Fig. 2. The average received aggregate interference power with the probabilistic LoS propagation model and the LoS ball models, where $H_D = 150$ m and $R_{\mathcal{B}} = 340$ m.

of the LoS ball model. In addition, to facilitate the analysis, the Poisson hard core process is approximated by a PPP with the same density [38].

Then, we have

$$\mathcal{P}_{SCD}^B \approx \sum_{m=0}^{M-1} \mathbb{E}_{r_b} \left[\sum_{p=0}^{m} \binom{m}{p} \frac{(-1)^p s^m e^{-sI_D}}{m! I_D^{p-m}} \mathcal{L}_{I_B}^{(p)}(s) \right], \tag{30}$$

Where $\mathbb{E}[I^p e^{-sI}] = (-1)^p \mathcal{L}_I^{(p)}(s)$ is used in (30), and $\mathcal{L}_I(s)$ is the Laplace transform of I. Then, we derive an approximated closed-form results for the conditional SCD probability that is efficient to compute.

Theorem 2: The conditional successful content delivery probability when the typical user associates with TBS is approximated by

$$\mathcal{P}_{SCD}^B \approx \sum_{m=0}^{M-1} \sum_{p=0}^{m} \frac{(\pi\lambda_B)^{p+1} \Upsilon}{p!(m-p)!} e^{\pi\lambda_B H_B^2} \left\| \mathbf{Q}_M^p \right\|_1, \tag{31}$$

where

$$\Upsilon = \int_{H_B}^{\infty} f_{r_b|B}(r) r^{2p} \varpi_d^{m-p} e^{-\pi\lambda_B k_0 r^2 - \varpi_d} dr \tag{32}$$

and

$$\varpi_d = \frac{\pi\bar{\gamma}\lambda_D K P_D}{c_B P_B} \Xi(r) r^{\alpha_B}. \tag{33}$$

$$\Xi(r) = \begin{cases} 2c_L \left(\ln R_{\mathcal{B}} - \ln \sqrt{r^2 + \Delta_H^2} \right) \\ + \frac{\delta_N c_N}{1-\delta_N} \left(R_{\mathcal{B}}^{2-\alpha_N} - R_o^{2-\alpha_N} \right), & \text{if } \alpha_L = 2, \\ \frac{\delta_L c_L}{1-\delta_L} \left((r^2 + \Delta_H^2)^{1-\frac{\alpha_L}{2}} - R_{\mathcal{B}}^{2-\alpha_L} \right) \\ + \frac{\delta_N c_N}{1-\delta_N} \left(R_{\mathcal{B}}^{2-\alpha_N} - R_o^{2-\alpha_N} \right), & \text{if } \alpha_L > 2. \end{cases} \tag{34}$$

Note that $f_{r_b|B}(r)$ is the PDF of the nearest distance derived from (24), $\Xi(r)$ is given in (34), with $\Delta_H^2 = H_D^2 - H_B^2$, and the

Toeplitz matrix is given by

$$\mathbf{Q}_M = \begin{bmatrix} 0 & & & & \\ k_1 & 0 & & & \\ k_2 & k_1 & 0 & & \\ \vdots & \vdots & & \ddots & \\ k_{M-1} & k_{M-2} & \dots & k_1 & 0 \end{bmatrix}. \tag{35}$$

Note that k_0 and k_i are given by

$$k_0 = V_K \bar{\gamma}^{\delta} + \frac{\delta_B \varphi_0(K, \bar{\gamma})}{(K+\delta_B)\bar{\gamma}^K}, \tag{36}$$

and

$$k_i = \binom{K-1+i}{K-1} \frac{\delta_B \bar{\gamma}^i \varphi_i(K, \bar{\gamma})}{i - \delta_B}, \tag{37}$$

respectively.

Proof: See Appendix C. ∎

The analytical result in Theorem 2 is rather cumbersome for analysis, thus we conduct asymptotic analysis to obtain some insights. We take $\alpha_L > 2$ as an example, and define $\Xi_L = \pi\lambda_D P_D \frac{\delta_L c_L}{1-\delta_L}, \Xi_{\mathcal{B}} = \Xi_L R_{\mathcal{B}}^{2-\alpha_L}, \Xi_b = \pi\lambda_B P_B \frac{\delta_B c_B}{1-\delta_B}$, then we can obtain the following corollary.

Corollary 3: The asymptotic conditional successful content delivery probability is approximated by

$$\mathcal{P}_{SCD}^{B,\text{asym}} \approx F_{r_b|B}(r_o), \tag{38}$$

where

$$r_o = \sqrt{\frac{M P_B c_B}{K\bar{\gamma} A_{b2}} - \frac{\Delta_{b0}}{A_{b2}} + \frac{\Delta_{b1}^2}{4\,A_{b2}^2}} - \frac{\Delta_{b1}}{2A_{b2}}, \tag{39}$$

with $\Delta_{b1} = A_{b1} - 2H_B A_{b2}$, and $\Delta_{b0} = A_{b0} - H_B A_{b1} + H_B^2 A_{b2}$, and A_{b0}, A_{b1}, A_{b2} are given by (40), (41), and (42), respectively.

$$A_{b0} = \Xi_b H_B^2 + \Xi_L H_B^{\alpha_B} H_D^{2-\alpha_L} + \Xi_{\mathcal{B}} H_B^{\alpha_B}, \tag{40}$$

$$\begin{aligned} A_{b1} = {} & 2\Xi_b H_B + \alpha_B \Xi_L H_B^{\alpha_B - 1} H_D^{2-\alpha_L} \\ & + (2-\alpha_L)\Xi_L H_B^{\alpha_B+1} H_D^{-\alpha_L} + \alpha_B \Xi_{\mathcal{B}} H_B^{\alpha_B - 1}, \end{aligned} \tag{41}$$

$$\begin{aligned} A_{b2} = {} & \Xi_L H_B^{\alpha_B} H_D^{-\alpha_L} \left(\alpha_B(\alpha_B-1)H_B^{-2}H_D^2 + \alpha_B(2-\alpha_L)\right. \\ & \left. + (\alpha_B+1)(2-\alpha_L) - \alpha_L(2-\alpha_L)H_B^2 H_D^{-2}\right) \\ & + 2\Xi_b + \alpha_B(\alpha_B-1)\Xi_{\mathcal{B}} H_B^{\alpha_B-2}. \end{aligned} \tag{42}$$

Proof: Since $\lim_{M\to\infty} \frac{1}{M}|\mathbf{h}_{000}\mathbf{w}_{00}|^2 = 1$, we have

$$\begin{aligned} \mathcal{P}_{SCD}^{B,\text{asym}} &= \mathbb{P}\left(M \geq s(I_B + I_D)\right) \\ &= \mathbb{P}\left(I_B \leq \frac{M}{s} - I_D\right) \\ &\approx \mathbb{P}\left(\bar{I}_B \leq \frac{M}{s} - \bar{I}_D\right), \end{aligned} \tag{43}$$

where, in the last step, the interference power from TBS and UAV are replaced by its corresponding average value. Similar to (68), by using the Campbell's Theorem, the average received aggregate interference power of I_B can be calculated by

$$\bar{I}_B = \frac{\pi\lambda_B P_B c_B \delta_B}{1-\delta_B} r_b^{2-\alpha_B} = \Xi_b r_b^{2-\alpha_B}. \tag{44}$$

Since the LoS interference is much stronger than that of the NLoS link, the interference from the UAV will be dominated by the LoS interference. For the case of $\alpha_L > 2$, we have

$$\mathcal{P}_{SCD}^{B,\text{asym}} \approx \mathbb{P}\left(\Xi_b R_b^2 + \pi\lambda_D P_D R_b^{\alpha_B}\Xi(r_b) \leq \frac{M P_B c_B}{K\bar{\gamma}}\right). \tag{45}$$

To facilitate the analysis, we expand the polynomial of r_b in the left hand side of the inequality at the vicinity of H_B through the Taylor series expansion as

$$\begin{aligned} & \Xi_b R_b^2 + \Xi_L R_b^{\alpha_B}(R_b^2 + \Delta_H^2)^{1-\frac{\alpha_L}{2}} - \Xi_{\mathcal{B}} R_b^{\alpha_B} \\ & = A_{b0} + A_{b1}(r_b - H_B) + A_{b2}(r_b - H_B)^2 + o(r_b^2) \\ & \approx \Delta_{b2} R_b^2 + \Delta_{b1} r_b + \Delta_{b0}. \end{aligned} \tag{46}$$

Then, we have

$$\mathcal{P}_{SCD}^{B,\text{asym}} \approx \mathbb{P}\left(r_b \leq R_o\right) = F_{r_b|B}(R_o). \tag{47}$$

This completes the proof. ∎

Remark 1: The asymptotic results for the case $\alpha_L = 2$ can be obtained in a similar way.

Note that when $M = 1$, the laplace transform of the interference $\mathcal{L}_{I_B}(s)$ can be further simplified, then we have the following corollary.

Corollary 4: When the TBS is fully loaded, i.e., $N = K$, (31) can be further simplified as

$$\mathcal{P}_{SCD}^{B} \approx \pi\lambda_B e^{\pi\lambda_B H_B^2} \int_{H_B}^{\infty} f_{r_b|B}(r) e^{-\pi\lambda_B k_0 r^2 - \varpi_d} dr. \tag{48}$$

Based on (45) or (48), we can analyze the impact of the height and density of UAV on the SCD performance.

Property 1: The conditional successful content delivery probability is a decreasing function of λ_D, and an increasing function of H_D.

B. UE Associated With Cached UAV

When the typical user is associated with the UAV, and the requested content is stored at its cache, the UAV can directly send the content to the user. Then, the received SINR can be expressed as

$$\gamma_{D,0} = \frac{P_D L_a(r_d)}{I'_B + I'_D + \sigma^2}, \tag{49}$$

where σ^2 is the received noise power, and the interference term is given by

$$I'_B = \sum_{i\in\Phi_B} \sum_{k=0}^{K-1} \frac{P_B}{K} |\mathbf{g}_i \mathbf{w}_{ik}|^2 L(|X_{i00}|), \tag{50}$$

and

$$I'_D = \sum_{i\in\Phi_D\setminus\{0\}} P_D L_a(|Y_{i00}|). \tag{51}$$

Due to the probabilistic propagation model, we need to consider two cases whether the A2G link is in LoS or NLoS. Since the received SINR from the NLoS link is much weaker than that from the LoS link, the conditional SCD is dominant by the LoS case, and the NLoS case is ignored. Similar to the case with TBS association, we have

$$\begin{aligned}\mathcal{P}_{SCD}^{D,\text{hit}} &\approx \mathbb{P}\left(\frac{P_D c_L r_d^{-\alpha_L}}{I'_B + I'_D} \geq \tilde{\gamma}\right) \\ &\overset{(d)}{\approx} \mathbb{P}\left(u \geq \frac{\tilde{\gamma}(I'_B + I'_D)}{P_D c_L r_d^{-\alpha_L}}\right) \\ &= \mathbb{E}_{r_d}\mathbb{E}_{I'_B+I'_D}\left[e^{-t(I'_B+I'_D)}\right] \\ &= \mathbb{E}_{r_d}\left[e^{-t\bar{I}'_B}\mathcal{L}_{I'_D}(t)\right],\end{aligned} \tag{52}$$

where $\tilde{\gamma} = 2^{\frac{QK_d}{\tau}} - 1$. In step (d), we use a "dummy" exponential variable u with unit mean to approximate the constant number one. In addition, $t = \frac{\tilde{\gamma}}{P_D c_L} r_d^{\alpha_L}$. Then, following the procedures in Appendix C, we can derive Theorem 3, which is given as follows.

Theorem 3: The SCD probability, conditioning that the typical user is associated with the UAV and the requested content is cached in the UAV, is approximated by

$$\mathcal{P}_{SCD}^{D,\text{hit}} \approx \int_{H_D}^{R_{\mathcal{B}}} f_{r_d|D}(r) e^{-\pi\lambda_D \Upsilon_L(r)} e^{-\varpi_L r^{2+\alpha_L-\alpha_B}} dr, \tag{53}$$

where $f_{r_d|D}(r)$ is the PDF of the nearest distance derived from (25), $\varpi_L = \frac{\Xi_b \tilde{\gamma}}{P_D c_L}$, and $\Upsilon_L(r)$ is given as follows. When $\alpha_L > 2$, we have

$$\begin{aligned}\Upsilon_L(r) &= r^2\left({}_2F_1\left(-\delta_L, 1; 1-\delta_L; -\tilde{\gamma}\right) - 1\right) \\ &\quad - R_{\mathcal{B}}^2\left({}_2F_1\left(-\delta_L, 1; 1-\delta_L; -\frac{r^2\tilde{\gamma}}{R_{\mathcal{B}}^2}\right) - 1\right),\end{aligned} \tag{54}$$

when $\alpha_L = 2$, we have

$$\Upsilon_L(r) = \tilde{\gamma} r^2 \ln\left(R_{\mathcal{B}}^2\left(1 + \frac{r^2\tilde{\gamma}}{R_{\mathcal{B}}^2}\right)\right) - \ln r^2(1+\tilde{\gamma}). \tag{55}$$

Based on (53), we can obtain the following property.

Property 2: The conditional SCD probability first increases and then decreases with λ_D and H_D.

Proof: The strict mathematical proof is nontrivial due to the integration of high order terms in (53). From (25), we can find that $f_{r_d|D}$ is a decreasing function of H_D and an increasing function of λ_D, and the LoS ball radius is an increasing function of H_D, thus the above property can be proved. ■

C. UE Associated With the Uncached UAV

When the requested content is not stored in the cache, the UAV will first request it from the nearest TBS through the mmWave wireless backhaul, which will take T_b time period. Hence, the conditional SCD probability under the uncached UAV association is given by

$$\mathcal{P}_{SCD}^{D,\text{miss}} = \mathbb{P}\left(R \geq \frac{QK_d}{\tau - T_b}\right), \tag{56}$$

which can be derived from Theorem 3 by replacing $\tilde{\gamma}$ with $2^{\frac{QK_d}{\tau - T_b}} - 1$. We can find that the effect of backhaul transmission time maybe negligible when the size of the content is very small and the considered delivery time τ is very long.

TABLE I
UPA ANTENNA PATTERN [39]

Number of antennas	M
Half-power beamwidth (θ_B, θ_D)	$\sqrt{3}/\sqrt{M}$
Main-lobe gain (G_B, G_D)	M
Side-lobe gain (g_B, g_D)	$\frac{\sqrt{M}-\sqrt{3}M\sin(3\pi/(2\sqrt{M}))/2\pi}{\sqrt{M}-\sqrt{3}\sin(3\pi/(2\sqrt{M}))/2\pi}$

V. NUMERICAL RESULTS

In this section, we present the SCD performance through simulations to validate the theoretical analysis. We consider that the positions of the TBSs follow a HPPP process with density[5] $\lambda_B = 2/km^2$, and the height of each TBS is fixed as 10 m. The UAVs are dispatched to offload the traffic from the TBSs, and the positions of the UAVs follow a Position hard core process with the safe distance R_{safe} being 10 m. The user downlink communication is operated at a frequency of 2.4 GHz with a bandwidth of 10 MHz and the mmWave backhaul link operates in 73 GHz with a bandwidth of 1 GHz. The path loss exponents are set to be $\alpha_B = 3.25, \alpha_L = 2.25, \alpha_N = 4$, respectively, and the A2G channel parameters are $B_a = B_b = 0.136$, $C_a = C_b = 11.95$ [13]. Besides, the path loss constant is set as $c_B = -18.4$ dB and $c_L = -25.6$ dB, respectively. Each TBS is considered to have $N = 6$ antennas, and serve K users simultaneously in the same frequency band with SDMA, while for the UAVs, K_d users are served through TDMA. For the mmWave backhaul, we assume that both the TBS and the UAV are equipped with uniform planar square array with $N_{mB} = 16$ antenna elements and $N_{mD} = 8$ antenna elements, respectively. The main-lobe, side-lobe, and beamwidth of the sectorized antenna pattern are set as Table I, which is the same as [39]. The path loss constant of the mmWave link is $c_M = -69.8$ dB, with the transmission power of the mmWave TBS being $P_m = 25$ dBm and path loss exponent $\alpha_M = 2$, unless specified otherwise. In addition, the noise power of the mmWave link is set as $\sigma_m^2 = -174 + 10\log_{10}(BW) + N_f$ with the noise figure $N_f = 10$ dB.

The transmitting power levels of the TBS and UAVs are $P_B = 45$ dBm, and $P_D = 38$ dBm, respectively, and the noise power for the user communication link is ignored. The total content is divided into $T = 10^5$ files, with the content popularity parameter being $\kappa = 1$, and the cache size at each UAV is $L = 10^3$.

We first show the conditional SCD probability in Fig. 3. We can observe from Fig. 3 that the approximated theoretical conditional SCD probability is very close to the simulation results, and the asymptotic results follow similar trend with the simulations, which validate the theoretical analysis in Section III. Moreover,

[5]The unit of the density of both TBS and UAVs is number per square meters, and the typical UAV density used in this simulation is around $10/km^2$, i.e., λ_D is around 10^{-5}.

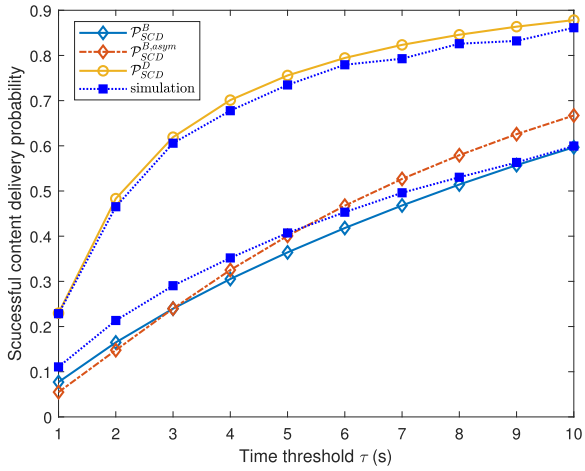

Fig. 3. The conditional SCD probability versus the transmission time threshold, where $K = 4$, $K_d = 1$, and $H_D = 100$ m.

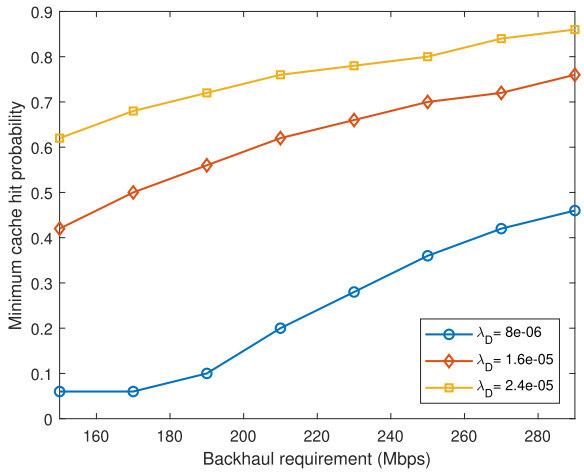

Fig. 5. The minimum cache hit probability requirement, where $P_m = 20$ dBm, $H_D = 150$ m, and $\alpha_M = 2$.

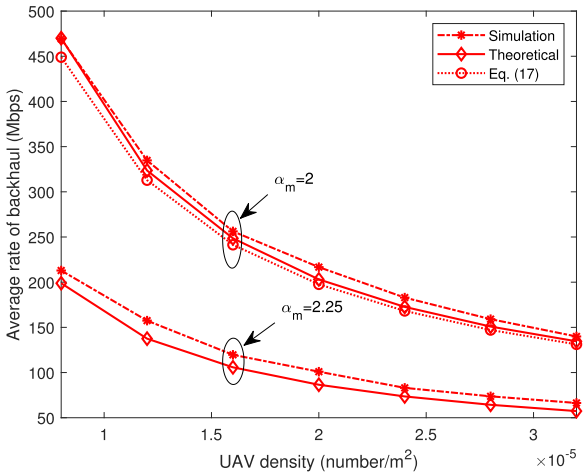

Fig. 4. The average rate of mmWave backhaul link, where $P_m = 25$ dBm and $H_D = 150$ m.

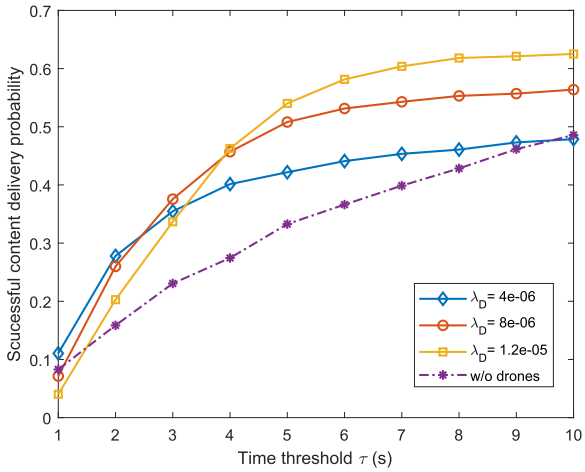

Fig. 6. The total SCD probability with different settings, where $Q = 20$ Mb, $P_m = 25$ dBm, $H_D = 100$ m, $\alpha_M = 2.25$, $L = 10^3$, $K = 6$, and $K_d = 2$.

we can observe that the conditional probability of SCD when the user is connected to the UAV is larger than that of the case associated with the cached TBS under the given system configurations, due to the LoS transmission. This also indicates that it is possible to enhance the probability of SCD by adding UAVs.

To investigate the feasibility of the mmWave wirelss backhaul, we then evaluate the average achievable rate of the mmWave wireless backhaul in Fig. 4. We can see that the approximated theoretical results are very close to the simulation results, and the closed-form expression for $\alpha_M = 2$ is very accurate. From Fig. 4, we can observe that high data rate backhaul up to hundreds of Mbps can be realized through the wireless mmWave link under the given system settings, which shows the feasibility of self-backhauling for UAVs. Notice that the backhaul rate decreases with the density of UAVs, i.e., the backhaul load, and the achievable rate decreases with the mmWave link path loss. Based on Corollary 2, we show the minimum cache hit probability requirement for given backhaul rate requirements in Fig. 5. We can observe from Fig. 5 that the minimum cache hit probability requirement increases as the backhaul rate requirements and the density of UAVs.

We then evaluate the total SCD probability, which is shown in Fig. 6. We can observe that the SCD probability increases as the required transmission time, and the caching-enabled UAV integrated network may outperform the conventional terrestrial network when the backhaul rate is high enough and the required transmission time is larger than a threshold. Specifically, the SCD probability can be improved up to 53%, when the required transmission time $\tau = 7$s, with the caching-enabled UAV integrated network as compared with the conventional terrestrial network. This answers our first question on the feasibility to deploy UAV networks to enhance the coverage. We can observe that when the density of UAV is very high and the required content delivery time is very short, adding UAVs into the terrestrial network may grant users more access opportunity at the cost of degrading the SCD performance.

The effect of the density of UAV on the SCD performance is also evaluated in Fig. 7. Clearly, the SCD performance first improves and then degrades as the increase of the density of UAVs,

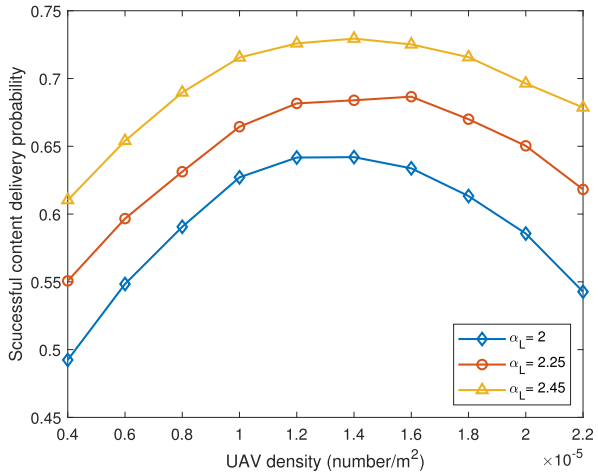

Fig. 7. The SCD probability versus the density of UAVs, where $Q = 20$ Mb, $\tau = 10$s, $H_D = 150$ m, $\alpha_M = 2.25$, $L = 10^3$, $K = 6$ and $K_d = 2$.

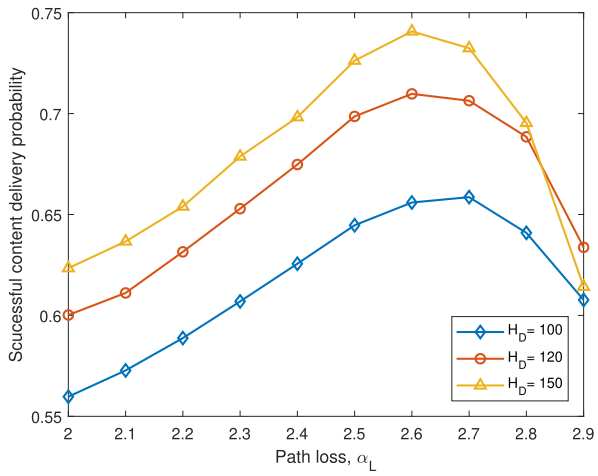

Fig. 8. The SCD probability versus path loss exponent, where $Q = 20$ Mb, $\tau = 10$s, $P_m = 25$ dBm, $\alpha_M = 2$, $L = 10^3$, $K = 6$ and $K_d = 2$.

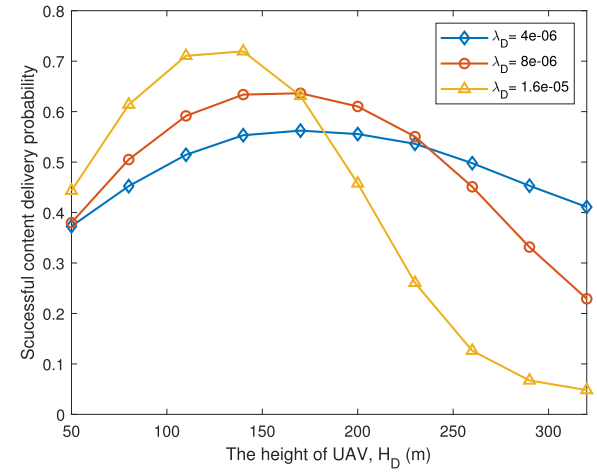

Fig. 9. The SCD probability versus the height of UAVs, $Q = 20$ Mb, $\tau = 10$s, $P_m = 25$ dBm, $\alpha_M = 2$, $L = 10^3$, $K = 6$ and $K_d = 2$.

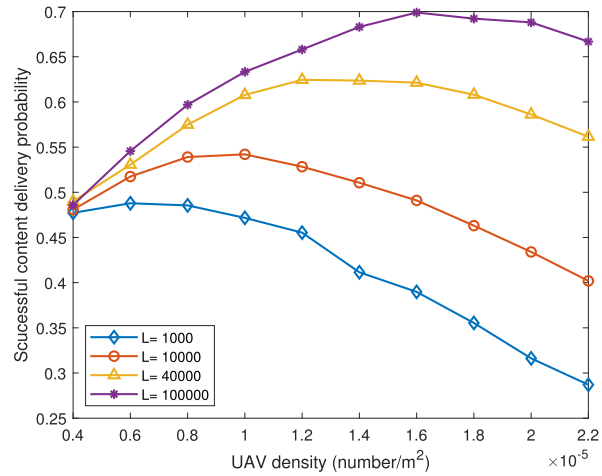

Fig. 10. The impact of finite cache on the SCD probability, where $Q = 20$ Mb, $\tau = 10$s, $H_D = 150$ m, $P_m = 32$ dBm, $\alpha_M = 2.45$, $\kappa = 0.5$, $K = 6$ and $K_d = 2$.

indicating that there exists an optimal UAV density maximizing the SCD performance. This is because, for the given system setting, the conditional probability of SCD for the UAV access link is better than that of the conventional terrestrial network, as shown in Fig. 3, by increasing the density of UAVs, the association probability to a UAV will be increased, which further improves the SCD performance. However, with the increase of the UAV density, the LoS interference increases much faster, resulting in a decrease in the conditional SCD.

The effect of path loss exponent and the height of UAVs on the SCD performance is also evaluated in Fig. 8 and Fig. 9, respectively. We can observe from Fig. 8 that the SCD probability is a concave function of the path loss exponent. This is because, on one hand, increasing α_L decreases the interference power, which improves the conditional SCD performance of the terrestrial network; on the other hand, the conditional SCD probability of the UAV network will be decreased by increasing α_L due to larger path loss. Moreover, from Fig. 9, we can observe that there exists an optimal height for the UAVs to maximize the SCD performance and the optimal height decreases as the increase of the density of UAVs. Therefore, UAV deployment and scheduling must be carefully designed to achieve the optimal performance.

Finally, we evaluate the impact of finite cache on the SCD performance in Fig. 10. We can see that the SCD performance can be improved by increasing the cache size for a given UAV density, due to the reduced backhaul requirement. However, for a given cache size, the SCD performance first increases and then decreases by increasing the UAV density. This is because, on one hand, the conditional SCD probability of the UAV network is a concave function of the UAV density, as shown in Fig. 7; on the other hand, the backhaul load increases as the UAV density and longer time is required for backhaul transmission when the UAV density is very high, which limits the SCD performance. Moreover, we find that there exists a large gap in the SCD performance with limited cache and that of the unlimited cache case ($L = 10^5$ corresponding to the infinite cache case since the total file size is 10^5), when the density of UAVs is very high.

VI. Conclusion

In this paper, we have evaluated the SCD performance in the UAV integrated terrestrial cellular network, where the caching-enabled UAVs are dispatched to offload the temporal traffic in congestion areas. We have derived the closed-form expression of the achievable rate of the mmWave wireless backhaul, and obtained the minimum cache hit probability to achieve a required backhaul rate. The closed-form expressions of the approximated conditional SCD probability have been derived by adopting a LoS ball model. It has been shown that up to 53% improvement in the SCD performance can be achieved with the integrated network as compared with the conventional terrestrial network. Moreover, there exists an optimal height and density of UAVs to maximize the SCD performance, and increasing the cache size is an effective way to improve the SCD performance when the density of UAVs is very high. The theoretical analysis in this paper provides some useful guidelines for the UAV deployment in the future UAV-assisted networks. In the future, we will consider the optimal deployment and resource scheduling to further improve the SCD performance.

Appendix A
Proof of Theorem 1

Denote $I_m = \sum_{j\in\Phi_B\setminus\{0\}} P_m G_j L_b(Z_{j0})$, based on the lemma in [32], for a given r_v, the average rate of the mmWave backhaul link can be calculated as

$$\begin{aligned}\bar{R}_b(r_v) &= \mathbb{E}_{\Phi_B^a}\left[\log\left(1+\frac{P_m G_S L_b(Z_{00})}{I_m+\sigma_m^2}\right)\middle| r_v\right]\\ &= \int_0^\infty \frac{1-\mathbb{E}[e^{-zP_m G_S c_M R_v^{-\alpha_M}}]}{z\ln 2}\mathbb{E}\left[e^{-z(I_m+\sigma_m^2)}\right]dz.\end{aligned} \tag{57}$$

The interference term can be characterized by

$$\begin{aligned}&\mathbb{E}\left[e^{-zI_m}\right]\\ &= \mathbb{E}\left[e^{-z\left(\sum_{i\in\Phi_B^a\setminus\{0\}} P_m G_j L_b(Z_{j0})\right)}\right]\\ &\overset{(a)}{=} \mathbb{E}\left[e^{-z\left(\sum_{i\in\Phi_B^a\setminus\{0\}} vP_m G_j L_b(Z_{j0})\right)}\right]\\ &\overset{(b)}{=} \mathbb{E}\left[\prod_{i\in\Phi_B^a\setminus\{0\}}\frac{1}{\left(1+\frac{zP_m\bar{G}_I c_M}{N_v R^{\alpha_M}}\right)^{N_v}}\right]\\ &\overset{(c)}{=} \exp\left(-\pi\lambda_B p_a\int_{R_v^2}^\infty\left(1-\frac{1}{\left(1+\frac{zP_m\bar{G}_I c_M}{N_v R^{\frac{\alpha_M}{2}}}\right)^{N_v}}\right)dR\right),\end{aligned} \tag{58}$$

where in step (a), we use a dummy variable v to represent the constant one, (b) holds due to the Gamma distribution of v, and (c) follows from the probability generating functional (PGFL) of PPP. With the results in [40], we can obtain Θ in (14) and (15).

Then by averaging $\bar{R}_b(r_v)$ over r_v, we can obtain the average backhaul rate.

Appendix B
Proof of Lemma 2

As per the nearest BS association rule, we have

$$\begin{aligned}\mathbb{P}(r_b\le r\mid r_b\le r_d) &= \frac{\mathbb{P}(r_b\le r, r_b\le r_d)}{\mathbb{P}(r_b\le r_d)}\\ &= \frac{\mathbb{P}(r_b\le r, r_b\le r_d)}{\mathcal{A}_B}.\end{aligned} \tag{59}$$

The joint probability can be calculated by

$$\mathbb{P}(r_b\le r, r_b\le r_d) = \int_0^r \mathbb{P}(r_d\ge r) f_{r_b}(r)dr. \tag{60}$$

When $r < H_D$, we have

$$\mathbb{P}(r_b\le r, r_b\le r_d) = F_{r_b}(r) = 1-e^{-\pi\lambda_B(r^2-H_B^2)}, \tag{61}$$

and when $r > H_D$, we have

$$\begin{aligned}&\mathbb{P}(r_b\le r, r_b\le r_d)\\ &= \int_0^{H_D} f_{r_b}(r)dr + \int_{H_D}^r \mathbb{P}(r_d\ge r) f_{r_b}(r)dr\\ &= 1-e^{-\pi\lambda_B(H_D^2-H_B^2)} + \int_{H_D}^r F_{r_d}(r) f_{r_b}(r)dr.\end{aligned} \tag{62}$$

Using the CDF in Lemma 1, Lemma 2 can be obtained.

Appendix C
Proof of Theorem 2

Define $g_i = \sum_{k=0}^{K-1} |\mathbf{h}_{i00}\mathbf{w}_i^{(k)}|^2$, $w = \frac{P_B c_B}{K}s$, then we can find that g_i follows a Gamma distribution with shape parameter K, then the Laplace transform of I_B can be expressed as

$$\begin{aligned}\mathcal{L}_{I_B}(s) &= \mathbb{E}_{I_B}\left[\exp\left(-\sum_{i\in\Phi_B\setminus\{0\}} wg_i\,|X_{i00}|^{-\alpha_B}\right)\right]\\ &= \mathbb{E}_{\Phi_B\setminus\{0\}}\left[\prod_{i\in\Phi_B\setminus\{0\}}\mathbb{E}_{g_i}\left[\exp(-wg_i\,|X_{i00}|^{-\alpha_B})\right]\right]\\ &\overset{(d)}{=} \exp\left(-\int_{\mathbb{R}^2}\left(1-\frac{1}{(1+wR^{-\alpha_B})^K}\right)\Lambda(dR)\right)\\ &= \exp\left(-\pi\lambda_B\int_{R_b^2}^\infty\left(1-\frac{1}{(1+wR^{-\frac{\alpha_B}{2}})^K}\right)dR\right),\end{aligned} \tag{63}$$

where (d) comes from the PGFL of PPP. By using eq. (8) in [41] and [35, eq. (3.194.2)], we have

$$\begin{aligned}\mathcal{L}_{I_B}(s) &= V_K(wP_B)^{\delta_B} - 1\\ &\quad + \delta_B\frac{{}_2F_1(K, K+\delta_B;\, K-\delta+1;\, -\frac{1}{wR_b^{-\alpha_B}})}{(K+\delta_B)(wR_b^{-\alpha_B})^K}.\end{aligned} \tag{64}$$

From (63), the p-th derivative of $\mathcal{L}_{I_B}(s)$ can be expressed in a recursive form given by [33]

$$\mathcal{L}_{I_B}^{(p)}(s) = \pi\lambda_B \sum_{i=0}^{p-1} \binom{p-1}{i} \frac{(K-1+p-i)!}{(K-1)!} \mathcal{L}_{I_B}^{(i)}(s) \times \int_{R_b^2}^{\infty} \frac{(-1)^{p-i}(c_B P_B R^{-\frac{\alpha_B}{2}})^{p-i}}{K^{p-i}(1+wR^{-\frac{\alpha_B}{2}})^{K+p-i}} dR. \quad (65)$$

Let $x_p = (-1)^p s^p / p! \mathcal{L}_{I_B}^{(p)}(s)$ and use the variable transformation $R^{-\frac{\alpha_B}{2}} \to v$ we have

$$x_p = \pi\lambda_B \delta_B \sum_{i=0}^{p-1} \frac{p-i}{p} \frac{(K-1+p-i)!}{(K-1)!} \times \int_0^{R_b^{-\alpha_B}} \frac{v^{p-i-\delta-1}}{(1+wv)^{p-i+K}} dv x_i. \quad (66)$$

With some mathematical manipulations, we can obtain

$$x_p = \pi\lambda_B R_b^2 \sum_{i=0}^{p-1} \frac{p-i}{p} k_{p-i} x_i, \quad (67)$$

where k_i is given by (37).

For the interference from other UAVs, by using the Campbell's theorem [36] and the LoS ball model, we have

$$\begin{aligned} \bar{I}_D &= \mathbb{E}[I_D] = \mathbb{E}\left[\sum_{j\in\Phi_D} P_D Y_{i0}^{(0)}\right] \\ &= \int_{\mathbb{R}^2} P_D \left(\mathbb{P}_L(R) c_L R^{-\alpha_L} + \mathbb{P}_N(R) c_N R^{-\alpha_N}\right) \Lambda(dR) \\ &= \int_{\sqrt{R_b^2+\Delta_H^2}}^{R_{\mathcal{B}}} 2\pi\lambda_D P_D c_L R^{1-\alpha_L} dR \\ &\quad + \int_{R_{\mathcal{B}}}^{R_o} 2\pi\lambda_D P_D c_N R^{1-\alpha_N} dR. \end{aligned} \quad (68)$$

By replacing the interference from UAV by its average value, the SCD probability can be calculated by

$$\begin{aligned} \mathcal{P}_{SCD}^B &\approx \sum_{m=0}^{M-1} \sum_{p=0}^{m} \mathbb{E}_{r_b}\left[e^{-s\bar{I}_D} \frac{(s\bar{I}_D)^{m-p}}{(m-p)!} x_p\right] \\ &= \sum_{m=0}^{M-1} \sum_{p=0}^{m} \mathbb{E}_{r_b}\left[\frac{e^{-s\bar{I}_D}(s\bar{I}_D)^{m-p}}{(m-p)!p!} \left\|a^p x_0 \mathbf{Q}_M^p\right\|_1\right], \end{aligned} \quad (69)$$

where $x_0 = \exp(-\pi\lambda_B k_0 R_b^2)$, and $a = \pi\lambda_B R_b^2$. The detailed derivation may refer to Appendix-A of [31].

Combining the above results, we can obtain Theorem 2.

REFERENCES

[1] W. Chen, J. Liu, H. Guo, and N. Kato, "Toward robust and intelligent drone swarm: Challenges and future directions," *IEEE Netw.*, vol. 34, no. 4, pp. 278–283, July/Aug. 2020.

[2] X. Zhou, S. Durrani, J. Guo, and H. Yanikomeroglu, "Underlay drone cell for temporary events: Impact of drone height and aerial channel environments," *IEEE Internet Things J.*, vol. 6, no. 2, pp. 1704–1718, Apr. 2019.

[3] Y. Huo, X. Dong, T. Lu, W. Xu, and M. Yuen, "Distributed and multilayer UAV networks for next-generation wireless communication and power transfer: A feasibility study," *IEEE Internet Things J.*, vol. 6, no. 4, pp. 7103–7115, Aug. 2019.

[4] B. Galkin, J. Kibilda, and L. A. Dasilva, "A stochastic model for UAV networks positioned above demand hotspots in urban environments," *IEEE Trans. Veh. Technol.*, vol. 68, no. 7, pp. 6985–6996, Jul. 2019.

[5] A. Asheralieva and D. Niyato, "Game theory and lyapunov optimization for cloud-based content delivery networks with device-to-device and uav-enabled caching," *IEEE Trans. Veh. Technol.*, vol. 68, no. 10, pp. 10 094–10 110, Oct. 2019.

[6] S. A. R. Naqvi, S. A. Hassan, H. Pervaiz, and Q. Ni, "Drone-aided communication as a key enabler for 5 G and resilient public safety networks," *IEEE Commun. Mag.*, vol. 56, no. 1, pp. 36–42, Jan. 2018.

[7] A. Al-Hourani, S. Kandeepan, and S. Lardner, "Optimal LAP altitude for maximum coverage," *IEEE Wireless Commun. Lett.*, vol. 3, no. 6, pp. 569–572, Dec. 2014.

[8] Y. Zhu, G. Zheng, and M. Fitch, "Secrecy rate analysis of UAV-enabled mmwave networks using matérn hardcore point processes," *IEEE J. Sel. Areas Commun.*, vol. 36, no. 7, pp. 1397–1409, Jul. 2018.

[9] W. Wu, N. Zhang, N. Cheng, Y. Tang, K. Aldubaikhy, and X. Shen, "Beef up mmWave dense cellular networks with D2D-assisted cooperative edge caching," *IEEE Trans. Veh. Technol.*, vol. 68, no. 4, pp. 3890–3904, Apr. 2019.

[10] H. Zhou, N. Cheng, J. Wang, J. Chen, Q. Yu, and X. Shen, "Toward dynamic link utilization for efficient vehicular edge content distribution," *IEEE Trans. Veh. Technol.*, vol. 68, no. 9, pp. 8301–8313, Sep. 2019.

[11] M. Mozaffari, W. Saad, M. Bennis, Y.-H. Nam, and M. Debbah, "A tutorial on UAVs for wireless networks: Applications, challenges, and open problems," *IEEE Commun. Surveys Tut.*, vol. 21, no. 3, pp. 2334–2360, *Jul.-Sep.*2019.

[12] M. Chen, M. Mozaffari, W. Saad, C. Yin, M. Debbah, and C. S. Hong, "Caching in the sky: Proactive deployment of cache-enabled unmanned aerial vehicles for optimized quality-of-experience," *IEEE J. Sel. Areas Commun.*, vol. 35, no. 5, pp. 1046–1061, May 2017.

[13] M. Mozaffari, W. Saad, M. Bennis, and M. Debbah, "Unmanned aerial vehicle with underlaid device-to-device communications: Performance and tradeoffs," *IEEE Trans. Wireless Commun.*, vol. 15, no. 6, pp. 3949–3963, Jun. 2016.

[14] V. V. Chetlur and H. S. Dhillon, "Downlink coverage analysis for a finite 3-D wireless network of unmanned aerial vehicles," *IEEE Trans. Commun.*, vol. 65, no. 10, pp. 4543–4558, Oct. 2017.

[15] X. Wang, H. Zhang, Y. Tian, and V. C. Leung, "Modeling and analysis of aerial base station-assisted cellular networks in finite areas under LoS and NLoS propagation," *IEEE Trans. Wireless Commun.*, vol. 17, no. 10, pp. 6985–7000, Oct. 2018.

[16] H. Wu, X. Tao, N. Zhang, and X. Shen, "Cooperative UAV cluster-assisted terrestrial cellular networks for ubiquitous coverage," *IEEE J. Sel. Areas Commun.*, vol. 36, no. 9, pp. 2045–2058, Sep. 2018.

[17] J. Liu, M. Sheng, R. Lyu, and J. Li, "Performance analysis and optimization of UAV integrated terrestrial cellular network," *IEEE Internet Things J.*, vol. 6, no. 2, pp. 1841–1855, Apr. 2019.

[18] M. Khabbaz, J. Antoun, and C. Assi, "Modeling and performance analysis of UAV-assisted vehicular networks," *IEEE Trans. Veh. Technol.*, vol. 68, no. 9, pp. 8384–8396, Sep. 2019.

[19] X. Lin *et al.*, "The sky is not the limit: LTE for unmanned aerial vehicles," *IEEE Commun. Mag.*, vol. 56, no. 4, pp. 204–210, Apr. 2018.

[20] M. Gapeyenko, V. Petrov, D. Moltchanov, S. Andreev, N. Himayat, and Y. Koucheryavy, "Flexible and reliable UAV-assisted backhaul operation in 5 G mmWave cellular networks," *IEEE J. Sel. Areas Commun.*, vol. 36, no. 11, pp. 2486–2496, Nov. 2018.

[21] Y. Huo and X. Dong, "Millimeter-wave for unmanned aerial vehicles networks: Enabling multi-beam multi-stream communications," 2018, *arXiv:1810.06923*.

[22] "Service Requirements for the 5G System," 3GPP TS 22.261 version 15.7.0 Release 15, Mar. 2019. [Online]. Available: https://www.3gpp.org/791DynaReport/22261.htm.

[23] S. Zhang, N. Zhang, P. Yang, and X. Shen, "Cost-effective cache deployment in mobile heterogeneous networks," *IEEE Trans. Veh. Technol.*, vol. 66, no. 12, pp. 11 264–11 276, Dec. 2017.

[24] Z. Chen, J. Lee, T. Q. Quek, and M. Kountouris, "Cooperative caching and transmission design in cluster-centric small cell networks," *IEEE Trans. Wireless Commun.*, vol. 16, no. 5, pp. 3401–3415, May 2017.
[25] L. Wang, K.-K. Wong, S. Lambotharan, A. Nallanathan, and M. Elkashlan, "Edge caching in dense heterogeneous cellular networks with massive MIMO-aided self-backhaul," *IEEE Trans. Wireless Commun.*, vol. 17, no. 9, pp. 6360–6372, Sep. 2018.
[26] G. Lee, Y. Sung, and J. Seo, "Randomly-directional beamforming in millimeter-wave multiuser MISO downlink," *IEEE Trans. Wireless Commun.*, vol. 15, no. 2, pp. 1086–1100, Feb. 2016.
[27] T. S. Rappaport *et al.*, "Millimeter wave mobile communications for 5 G cellular: It will work!," *IEEE Access*, vol. 1, pp. 335–349, 2013.
[28] J. G. Andrews, T. Bai, M. N. Kulkarni, A. Alkhateeb, A. K. Gupta, and R. W. Heath, "Modeling and analyzing millimeter wave cellular systems," *IEEE Trans. Commun.*, vol. 65, no. 1, pp. 403–430, Jan. 2017.
[29] B. Galkin, J. Kibilda, and L. A. DaSilva, "Backhaul for low-altitude UAVs in urban environments," in *Proc. IEEE Int. Conf. Commun.*, Kansas City, MO, USA, 2018, pp. 1–6.
[30] C.-H. Liu and L.-C. Wang, "Optimal cell load and throughput in green small cell networks with generalized cell association," *IEEE J. Sel. Areas Commun.*, vol. 34, no. 5, pp. 1058–1072, May 2016.
[31] C. Li, J. Zhang, and K. B. Letaief, "Throughput and energy efficiency analysis of small cell networks with multi-antenna base stations," *IEEE Trans. Wireless Commun.*, vol. 13, no. 5, pp. 2505–2517, May 2014.
[32] K. A. Hamdi, "A useful lemma for capacity analysis of fading interference channels," *IEEE Trans. Commun.*, vol. 58, no. 2, pp. 411–416, Feb. 2010.
[33] W. Wang, K. C. Teh, and K. Li, "Artificial noise aided physical layer security in multi-antenna small-cell networks," *IEEE Trans. Inf. Forensics Secur.*, vol. 12, no. 6, pp. 1470–1482, Jun. 2017.
[34] J. G. Andrews, F. Baccelli, and R. K. Ganti, "A tractable approach to coverage and rate in cellular networks," *IEEE Trans. Commun.*, vol. 59, no. 11, pp. 3122–3134, Nov. 2011.
[35] I. Gradshteyn, I. Ryzhik, A. Jeffrey, D. Zwillinger, and S. Technica, *Table of Integrals, Series, and Products*. New York, NY, USA: Academic Press, 2007.
[36] M. Haenggi, *Stochastic Geometry for Wireless Networks*. Cambridge, U.K.: Cambridge Univ. Press, 2012.
[37] X. Yu, J. Zhang, R. Schober, and K. B. Letaief, "A tractable framework for coverage analysis of cellular-connected UAV networks," in *Proc. IEEE Int. Conf. Commun. Workshops (ICC Workshops)*, Shanghai, China, 2019, pp. 1–6.
[38] W. Wang, K. C. Teh, K. H. Li, and S. Luo, "On the impact of adaptive eavesdroppers in multi-antenna cellular networks," *IEEE Trans. Inf. Forensics Secur.*, vol. 13, no. 2, pp. 269–279, Feb. 2018.
[39] K. Venugopal, M. C. Valenti, and R. W. Heath, "Device-to-device millimeter wave communications: Interference, coverage, rate, and finite topologies," *IEEE Trans. Wireless Commun.*, vol. 15, no. 9, pp. 6175–6188, Sep. 2016.
[40] D. Liu and C. Yang, "Caching policy toward maximal success probability and area spectral efficiency of cache-enabled HetNets," *IEEE Trans. Commun.*, vol. 65, no. 6, pp. 2699–2714, Jun. 2017.
[41] M. Haenggi, J. G. Andrews, F. Baccelli, O. Dousse, and M. Franceschetti, "Stochastic geometry and random graphs for the analysis and design of wireless networks," *IEEE J. Sel. Areas Commun.*, vol. 27, no. 7, pp. 1029–1046, Sep. 2009.

Wei Wang (Member, IEEE) received the B.Eng. degree in information countermeasure technology and the M.Eng. degree in signal and information processing from Xidian University, Xi'an, China, in 2011 and 2014, respectively, and the Ph.D. degree in electrical and electronic engineering from Nanyang Technological University, Singapore, in 2018. From September 2018 to August 2019, he was a Postdoctoral Fellow with the Department of Electrical and Computer Engineering, University of Waterloo, Waterloo, ON, Canada. He is currently a Professor with the Nanjing University of Aeronautics and Astronautics, Nanjing, China. His research interests include wireless communications, space-air-ground integrated networks, wireless security, and blockchain. He was awarded the IEEE Student Travel Grants for IEEE ICC 2017 and the Chinese Government Award for outstanding self-financed students abroad.

Nan Cheng (Member, IEEE) received the B.E. and M.S. degrees from the Department of Electronics and Information Engineering, Tongji University, Shanghai, China, and the Ph.D. degree from the Department of Electrical and Computer Engineering, University of Waterloo, Waterloo, ON, Canada. He is currently a Joint Professor with the School of Telecommunication, Xidian University, Xi'an, China. He is also a Joint Postdoctoral Fellow with the Department of Electrical and Computer Engineering, University of Toronto, Toronto, ON, Canada, and with the Department of Electrical and Computer Engineering, University of Waterloo. His research interests include performance analysis, MAC, opportunistic communication for vehicular networks, unmanned aerial vehicles, and application of artificial intelligence for wireless networks.

Yiliang Liu (Member, IEEE) received the B.E and M.Sc. degrees in computer science and communication engineering, Jiangsu University, Zhenjiang, China, and the Ph.D. degree from the School of Electronics and Information Engineering, Harbin Institute of Technology, Harbin, China, in 2012, 2015, and 2020, respectively. From 2014 to 2015, he was a Visiting Research Student with the Department of Engineering Science, National Cheng Kung University, Tainan, Taiwan, and from 2018 to 2019, with the Department of Electrical and Computer Engineering, University of Waterloo, Waterloo, ON, Canada. He is currently a Lecturer with Xi'an Jiaotong University, Xi'an, China. His research interests include the security of wireless communications, physical layer security, and intelligent connected vehicles. He was the recipient of the Outstanding Doctoral Dissertation Award from China Education Society of Electronics in 2020 and the Best Paper Award of IEEE SYSTEMS JOURNAL in 2021.

Haibo Zhou (Senior Member, IEEE) received the Ph.D. degree in information and communication engineering from Shanghai Jiao Tong University, Shanghai, China, in 2014. From 2014 to 2017, he was a Postdoctoral Fellow with the Broadband Communications Research Group, Department of Electrical and Computer Engineering, University of Waterloo, Waterloo, ON, Canada. He is currently an Associate Professor with the School of Electronic Science and Engineering, Nanjing University, Nanjing, China. His research interests include resource management and protocol design in vehicular ad hoc networks, 5G or B5G wireless networks, and space–air–ground integrated networks. He was the recipient of the 2019 IEEE ComSoc Asia-Pacific Outstanding Young Researcher Award. He was the Invited Track Co-Chair for ICCC'2019, VTC-Fall'2020 and a TPC Member of many IEEE conferences, including GLOBECOM, ICC, and VTC. He is currently an Associate Editor for the IEEE INTERNET OF THINGS JOURNAL, *IEEE Network Magazine*, IEEE WIRELESS COMMUNICATIONS LETTER.

Xiaodong Lin (Fellow, IEEE) received the Ph.D. degree in information engineering from the Beijing University of Posts and Telecommunications, Beijing, China, in 1998, and the Ph.D. degree in electrical and computer engineering from the University of Waterloo, Waterloo, ON, Canada, in 2008. He is currently a Professor with the School of Computer Science, College of Engineering and Physical Sciences, University of Guelph, Guelph, ON, Canada. His research interests include wireless network security, applied cryptography, computer forensics, software security, and wireless networking and mobile computing. He was the recipient of the Outstanding Achievement in Graduate Studies Award from the University of Waterloo, the Canada Graduate Scholarship for Doctoral Award from the Natural Sciences and Engineering Research Council of Canada, and the Best Paper awards of the 18th International Conference on Computer Communications and Networks in 2009, the Fifth International Conference on Body Area Networks in 2010, and the IEEE International Conference on Communications in 2007.

Xuemin (Sherman) Shen (Fellow, IEEE) received the Ph.D. degree in electrical engineering from Rutgers University, New Brunswick, NJ, USA, in 1990. He is currently a University Professor with the Department of Electrical and Computer Engineering, University of Waterloo, Waterloo, ON, Canada. His research interests include network resource management, wireless network security, social networks, 5G and beyond, and vehicular ad hoc and sensor networks. He is a registered Professional Engineer of Ontario, Canada, an Engineering Institute of Canada Fellow, a Canadian Academy of Engineering Fellow, a Royal Society of Canada Fellow, a Chinese Academy of Engineering Foreign Fellow, and a Distinguished Lecturer of the IEEE Vehicular Technology Society and Communications Society.

Dr. Shen received the R.A. Fessenden Award in 2019 from IEEE, Canada, Award of Merit from the Federation of Chinese Canadian Professionals (Ontario) in 2019, the James Evans Avant Garde Award in 2018 from the IEEE Vehicular Technology Society, the Joseph LoCicero Award in 2015, the Education Award in 2017 from the IEEE Communications Society, and the Technical Recognition Award from Wireless Communications Technical Committee in 2019 and AHSN Technical Committee in 2013. He was also the recipient of the Excellent Graduate Supervision Award in 2006 from the University of Waterloo and the Premiers Research Excellence Award (PREA) in 2003 from the Province of Ontario, Canada. He was the Technical Program Committee Chair or Co-Chair for IEEE Globecom'16, IEEE Infocom'14, IEEE VTC'10 Fall, IEEE Globecom'07, and the Chair for the IEEE Communications Society Technical Committee on Wireless Communications. He was the elected IEEE Communications Society Vice President for Technical and Educational Activities, the Vice President for Publications, a Member-at-Large on the Board of Governors, the Chair of the Distinguished Lecturer Selection Committee, a Member of IEEE ComSoc Fellow Selection Committee. He was the Editor-in-Chief of the IEEE INTERNET OF THINGS JOURNAL, IEEE NETWORK, and *IET Communications*.